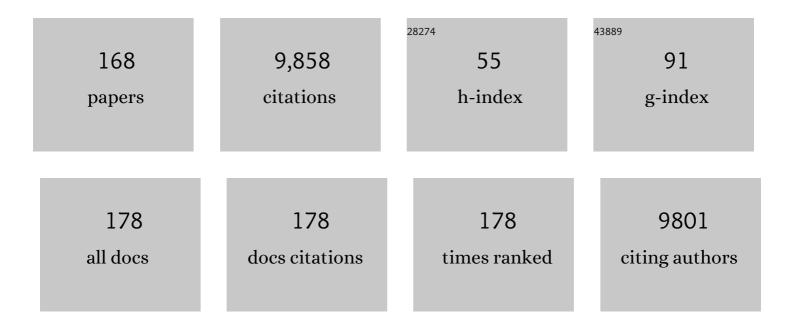
List of Publications by Year in descending order

Source: https://exaly.com/author-pdf/8067204/publications.pdf Version: 2024-02-01



FENC DINC

#	Article	IF	CITATIONS
1	Automated minimization of steric clashes in protein structures. Proteins: Structure, Function and Bioinformatics, 2011, 79, 261-270.	2.6	372
2	Eris: an automated estimator of protein stability. Nature Methods, 2007, 4, 466-467.	19.0	355
3	Ab Initio Folding of Proteins with All-Atom Discrete Molecular Dynamics. Structure, 2008, 16, 1010-1018.	3.3	287
4	Topological determinants of protein folding. Proceedings of the National Academy of Sciences of the United States of America, 2002, 99, 8637-8641.	7.1	278
5	Implications of peptide assemblies in amyloid diseases. Chemical Society Reviews, 2017, 46, 6492-6531.	38.1	262
6	Community-wide assessment of GPCR structure modelling and ligand docking: GPCR Dock 2008. Nature Reviews Drug Discovery, 2009, 8, 455-463.	46.4	260
7	Ab initio RNA folding by discrete molecular dynamics: From structure prediction to folding mechanisms. Rna, 2008, 14, 1164-1173.	3.5	258
8	Mechanism for the ?-helix to ?-hairpin transition. Proteins: Structure, Function and Bioinformatics, 2003, 53, 220-228.	2.6	252
9	<i>RNA-Puzzles</i> : A CASP-like evaluation of RNA three-dimensional structure prediction. Rna, 2012, 18, 610-625.	3.5	241
10	iFoldRNA: three-dimensional RNA structure prediction and folding. Bioinformatics, 2008, 24, 1951-1952.	4.1	200
11	Molecular Dynamics Simulation of Amyloid \hat{I}^2 Dimer Formation. Biophysical Journal, 2004, 87, 2310-2321.	0.5	194
12	Discrete Molecular Dynamics: An Efficient And Versatile Simulation Method For Fine Protein Characterization. Journal of Physical Chemistry B, 2012, 116, 8375-8382.	2.6	179
13	Emergence of Protein Fold Families through Rational Design. PLoS Computational Biology, 2006, 2, e85.	3.2	177
14	Engineered allosteric activation of kinases in living cells. Nature Biotechnology, 2010, 28, 743-747.	17.5	177
15	<i>RNA-Puzzles</i> Round II: assessment of RNA structure prediction programs applied to three large RNA structures. Rna, 2015, 21, 1066-1084.	3.5	161
16	RNA-Puzzles Round III: 3D RNA structure prediction of five riboswitches and one ribozyme. Rna, 2017, 23, 655-672.	3.5	158
17	Molecular Dynamics Simulation of the SH3 Domain Aggregation Suggests a Generic Amyloidogenesis Mechanism. Journal of Molecular Biology, 2002, 324, 851-857.	4.2	157
18	Modeling Backbone Flexibility Improves Protein Stability Estimation. Structure, 2007, 15, 1567-1576.	3.3	147

#	Article	IF	CITATIONS
19	Direct Molecular Dynamics Observation of Protein Folding Transition State Ensemble. Biophysical Journal, 2002, 83, 3525-3532.	0.5	133
20	Inhibition of amyloid beta toxicity in zebrafish with a chaperone-gold nanoparticle dual strategy. Nature Communications, 2019, 10, 3780.	12.8	132
21	Dynamical roles of metal ions and the disulfide bond in Cu, Zn superoxide dismutase folding and aggregation. Proceedings of the National Academy of Sciences of the United States of America, 2008, 105, 19696-19701.	7.1	131
22	Folding Trp-Cage to NMR Resolution Native Structure Using a Coarse-Grained Protein Model. Biophysical Journal, 2005, 88, 147-155.	0.5	130
23	Direct observation of a single nanoparticle–ubiquitin corona formation. Nanoscale, 2013, 5, 9162.	5.6	116
24	Rational design of a ligand-controlled protein conformational switch. Proceedings of the National Academy of Sciences of the United States of America, 2013, 110, 6800-6804.	7.1	111
25	Multiscale Modeling of Nucleosome Dynamics. Biophysical Journal, 2007, 92, 1457-1470.	0.5	104
26	Stabilizing Off-pathway Oligomers by Polyphenol Nanoassemblies for IAPP Aggregation Inhibition. Scientific Reports, 2016, 6, 19463.	3.3	104
27	On the significance of an RNA tertiary structure prediction. Rna, 2010, 16, 1340-1349.	3.5	103
28	Graphene quantum dots against human IAPP aggregation and toxicity <i>in vivo</i> . Nanoscale, 2018, 10, 19995-20006.	5.6	100
29	RNA-Puzzles Round IV: 3D structure predictions of four ribozymes and two aptamers. Rna, 2020, 26, 982-995.	3.5	100
30	Inhibition of hIAPP Amyloid Aggregation and Pancreatic β-Cell Toxicity by OH-Terminated PAMAM Dendrimer. Small, 2016, 12, 1615-1626.	10.0	99
31	Chemical and Biophysical Signatures of the Protein Corona in Nanomedicine. Journal of the American Chemical Society, 2022, 144, 9184-9205.	13.7	98
32	Molecular Origin of Polyglutamine Aggregation in Neurodegenerative Diseases. PLoS Computational Biology, 2005, 1, e30.	3.2	92
33	Discrete molecular dynamics. Wiley Interdisciplinary Reviews: Computational Molecular Science, 2011, 1, 80-92.	14.6	91
34	Protein folding: Then and now. Archives of Biochemistry and Biophysics, 2008, 469, 4-19.	3.0	88
35	Mitigation of Amyloidosis with Nanomaterials. Advanced Materials, 2020, 32, e1901690.	21.0	87
36	Polyglutamine Induced Misfolding of Huntingtin Exon1 is Modulated by the Flanking Sequences. PLoS Computational Biology, 2010, 6, e1000772.	3.2	86

#	Article	IF	CITATIONS
37	Rapid Flexible Docking Using a Stochastic Rotamer Library of Ligands. Journal of Chemical Information and Modeling, 2010, 50, 1623-1632.	5.4	80
38	Structural and Dynamic Determinants of Protein-Peptide Recognition. Structure, 2011, 19, 1837-1845.	3.3	79
39	Direct Observation of Protein Folding, Aggregation, and a Prion-like Conformational Conversion. Journal of Biological Chemistry, 2005, 280, 40235-40240.	3.4	77
40	Three-dimensional RNA structure refinement by hydroxyl radical probing. Nature Methods, 2012, 9, 603-608.	19.0	77
41	Discrete molecular dynamics simulations of peptide aggregation. Physical Review E, 2004, 69, 041908.	2.1	74
42	Local Unfolding of Cu, Zn Superoxide Dismutase Monomer Determines the Morphology of Fibrillar Aggregates. Journal of Molecular Biology, 2012, 421, 548-560.	4.2	74
43	Simple but predictive protein models. Trends in Biotechnology, 2005, 23, 450-455.	9.3	73
44	Topological Determinants of Protein Domain Swapping. Structure, 2006, 14, 5-14.	3.3	73
45	Fast complementation of split fluorescent protein triggered by DNA hybridization. Proceedings of the National Academy of Sciences of the United States of America, 2006, 103, 2052-2056.	7.1	73
46	Reconstruction of the src-SH3 Protein Domain Transition State Ensemble using Multiscale Molecular Dynamics Simulations. Journal of Molecular Biology, 2005, 350, 1035-1050.	4.2	72
47	Graphene oxide inhibits hIAPP amyloid fibrillation and toxicity in insulin-producing NIT-1 cells. Physical Chemistry Chemical Physics, 2016, 18, 94-100.	2.8	70
48	Native-like RNA Tertiary Structures Using a Sequence-Encoded Cleavage Agent and Refinement by Discrete Molecular Dynamics. Journal of the American Chemical Society, 2009, 131, 2541-2546.	13.7	65
49	Harnessing a Physiologic Mechanism for siRNA Delivery With Mimetic Lipoprotein Particles. Molecular Therapy, 2012, 20, 1582-1589.	8.2	65
50	Star Polymers Reduce Islet Amyloid Polypeptide Toxicity via Accelerated Amyloid Aggregation. Biomacromolecules, 2017, 18, 4249-4260.	5.4	65
51	New Insights into FAK Signaling and Localization Based on Detection of a FAT Domain Folding Intermediate. Structure, 2004, 12, 2161-2171.	3.3	62
52	β-barrel Oligomers as Common Intermediates of Peptides Self-Assembling into Cross-β Aggregates. Scientific Reports, 2018, 8, 10353.	3.3	62
53	Competitive Binding of Natural Amphiphiles with Graphene Derivatives. Scientific Reports, 2013, 3, 2273.	3.3	61
54	Folding of Cu, Zn Superoxide Dismutase and Familial Amyotrophic Lateral Sclerosis. Journal of Molecular Biology, 2003, 334, 515-525.	4.2	59

#	Article	IF	CITATIONS
55	Scaling Behavior and Structure of Denatured Proteins. Structure, 2005, 13, 1047-1054.	3.3	58
56	Mitigating Human IAPP Amyloidogenesis In Vivo with Chiral Silica Nanoribbons. Small, 2018, 14, e1802825.	10.0	57
57	Contrasting effects of nanoparticle–protein attraction on amyloid aggregation. RSC Advances, 2015, 5, 105489-105498.	3.6	56
58	Inhibition of IAPP aggregation by insulin depends on the insulin oligomeric state regulated by zinc ion concentration. Scientific Reports, 2015, 5, 8240.	3.3	50
59	Cofibrillization of Pathogenic and Functional Amyloid Proteins with Gold Nanoparticles against Amyloidogenesis. Biomacromolecules, 2017, 18, 4316-4322.	5.4	50
60	Amyloid Selfâ€Assembly of hIAPP8â€20 via the Accumulation of Helical Oligomers, αâ€Helix to βâ€5heet Transition, and Formation of βâ€Barrel Intermediates. Small, 2019, 15, e1805166.	10.0	49
61	Interaction of firefly luciferase and silver nanoparticles and its impact on enzyme activity. Nanotechnology, 2013, 24, 345101.	2.6	47
62	Amphiphilic surface chemistry of fullerenols is necessary for inhibiting the amyloid aggregation of alpha-synuclein NACore. Nanoscale, 2019, 11, 11933-11945.	5.6	47
63	Accelerated Amyloid Beta Pathogenesis by Bacterial Amyloid FapC. Advanced Science, 2020, 7, 2001299.	11.2	47
64	Novel application of a perturbed photonic crystal: High-quality filter. Applied Physics Letters, 1997, 71, 2889-2891.	3.3	46
65	Gaia: automated quality assessment of protein structure models. Bioinformatics, 2011, 27, 2209-2215.	4.1	44
66	Nucleation of β-rich oligomers and β-barrels in the early aggregation of human islet amyloid polypeptide. Biochimica Et Biophysica Acta - Molecular Basis of Disease, 2019, 1865, 434-444.	3.8	44
67	Spontaneous formation of β-sheet nano-barrels during the early aggregation of Alzheimer's amyloid beta. Nano Today, 2021, 38, 101125.	11.9	44
68	Structural and Thermodynamic Effects of Post-translational Modifications in Mutant and Wild Type Cu, Zn Superoxide Dismutase. Journal of Molecular Biology, 2011, 408, 555-567.	4.2	43
69	Computational approaches to understanding protein aggregation in neurodegeneration. Journal of Molecular Cell Biology, 2014, 6, 104-115.	3.3	43
70	NanoEHS beyond toxicity – focusing on biocorona. Environmental Science: Nano, 2017, 4, 1433-1454.	4.3	43
71	Distinct oligomerization and fibrillization dynamics of amyloid core sequences of amyloid-beta and islet amyloid polypeptide. Physical Chemistry Chemical Physics, 2017, 19, 28414-28423.	2.8	43
72	Active Nuclear Receptors Exhibit Highly Correlated AF-2 Domain Motions. PLoS Computational Biology, 2008, 4, e1000111.	3.2	42

#	Article	IF	CITATIONS
73	Effect of fullerenol surface chemistry on nanoparticle binding-induced protein misfolding. Nanoscale, 2014, 6, 8340-8349.	5.6	41
74	Identifying weak interdomain interactions that stabilize the supertertiary structure of the N-terminal tandem PDZ domains of PSD-95. Nature Communications, 2018, 9, 3724.	12.8	41
75	Understanding Effects of PAMAM Dendrimer Size and Surface Chemistry on Serum Protein Binding with Discrete Molecular Dynamics Simulations. ACS Sustainable Chemistry and Engineering, 2018, 6, 11704-11715.	6.7	41
76	The Length Dependence of the PolyQ-mediated Protein Aggregation. Journal of Biological Chemistry, 2007, 282, 25487-25492.	3.4	40
77	PAMAM Dendrimers and Graphene: Materials for Removing Aromatic Contaminants from Water. Environmental Science & Technology, 2015, 49, 4490-4497.	10.0	40
78	Islet Amyloid Polypeptide Promotes Amyloid-Beta Aggregation by Binding-Induced Helix-Unfolding of the Amyloidogenic Core. ACS Chemical Neuroscience, 2018, 9, 967-975.	3.5	39
79	Profiling the Serum Protein Corona of Fibrillar Human Islet Amyloid Polypeptide. ACS Nano, 2018, 12, 6066-6078.	14.6	39
80	Multiple Folding Pathways of the SH3 Domain. Biophysical Journal, 2004, 87, 521-533.	0.5	38
81	Modulating protein amyloid aggregation with nanomaterials. Environmental Science: Nano, 2017, 4, 1772-1783.	4.3	38
82	Incorporating Backbone Flexibility in MedusaDock Improves Ligand-Binding Pose Prediction in the CSAR2011 Docking Benchmark. Journal of Chemical Information and Modeling, 2013, 53, 1871-1879.	5.4	37
83	Binding of cytoskeletal proteins with silver nanoparticles. RSC Advances, 2013, 3, 22002.	3.6	36
84	Submillisecond Elastic Recoil Reveals Molecular Origins of Fibrin Fiber Mechanics. Biophysical Journal, 2013, 104, 2671-2680.	0.5	35
85	Nanoscale inhibition of polymorphic and ambidextrous IAPP amyloid aggregation with small molecules. Nano Research, 2018, 11, 3636-3647.	10.4	35
86	A structural model reveals energy transduction in dynein. Proceedings of the National Academy of Sciences of the United States of America, 2006, 103, 18540-18545.	7.1	34
87	Effects of Protein Corona on IAPP Amyloid Aggregation, Fibril Remodelling, and Cytotoxicity. Scientific Reports, 2017, 7, 2455.	3.3	34
88	Graphene quantum dots rescue protein dysregulation of pancreatic β-cells exposed to human islet amyloid polypeptide. Nano Research, 2019, 12, 2827-2834.	10.4	34
89	Amyloid Aggregation under the Lens of Liquid–Liquid Phase Separation. Journal of Physical Chemistry Letters, 2021, 12, 368-378.	4.6	34
90	Synthesis and in vitro properties of iron oxide nanoparticles grafted with brushed phosphorylcholine and polyethylene glycol. Polymer Chemistry, 2016, 7, 1931-1944.	3.9	32

#	Article	IF	CITATIONS
91	Amyloidosis inhibition, a new frontier of the protein corona. Nano Today, 2020, 35, 100937.	11.9	32
92	Robust and Generic RNA Modeling Using Inferred Constraints: A Structure for the Hepatitis C Virus IRES Pseudoknot Domain. Biochemistry, 2010, 49, 4931-4933.	2.5	31
93	Structural Basis for μ-Opioid Receptor Binding and Activation. Structure, 2011, 19, 1683-1690.	3.3	30
94	Thermostability and reversibility of silver nanoparticle–protein binding. Physical Chemistry Chemical Physics, 2015, 17, 1728-1739.	2.8	30
95	Parallel Folding Pathways in the SH3 Domain Protein. Journal of Molecular Biology, 2007, 373, 1348-1360.	4.2	29
96	Nâ€ŧerminal strands of filamin Ig domains act as a conformational switch under biological forces. Proteins: Structure, Function and Bioinformatics, 2010, 78, 12-24.	2.6	29
97	iFold: a platform for interactive folding simulations of proteins. Bioinformatics, 2006, 22, 2693-2694.	4.1	27
98	Promotion or Inhibition of Islet Amyloid Polypeptide Aggregation by Zinc Coordination Depends on Its Relative Concentration. Biochemistry, 2015, 54, 7335-7344.	2.5	27
99	Structures and dynamics of β-barrel oligomer intermediates of amyloid-beta16-22 aggregation. Biochimica Et Biophysica Acta - Biomembranes, 2018, 1860, 1687-1697.	2.6	27
100	Single-Molecular Heteroamyloidosis of Human Islet Amyloid Polypeptide. Nano Letters, 2019, 19, 6535-6546.	9.1	27
101	Hybrid Dynamics Simulation Engine for Metalloproteins. Biophysical Journal, 2012, 103, 767-776.	0.5	26
102	Nanosilver Mitigates Biofilm Formation via FapC Amyloidosis Inhibition. Small, 2020, 16, e1906674.	10.0	26
103	G Protein Mono-ubiquitination by the Rsp5 Ubiquitin Ligase. Journal of Biological Chemistry, 2009, 284, 8940-8950.	3.4	25
104	Inhibition of Amyloid Aggregation and Toxicity with Janus Iron Oxide Nanoparticles. Chemistry of Materials, 2021, 33, 6484-6500.	6.7	25
105	Physical and toxicological profiles of human IAPP amyloids and plaques. Science Bulletin, 2019, 64, 26-35.	9.0	24
106	Misfolding and Self-Assembly Dynamics of Microtubule-Binding Repeats of the Alzheimer-Related Protein Tau. Journal of Chemical Information and Modeling, 2021, 61, 2916-2925.	5.4	24
107	Fidelity of the Protein Structure Reconstruction from Inter-Residue Proximity Constraints. Journal of Physical Chemistry B, 2007, 111, 7432-7438.	2.6	23
108	Elevated amyloidoses of human IAPP and amyloid beta by lipopolysaccharide and their mitigation by carbon quantum dots. Nanoscale, 2020, 12, 12317-12328.	5.6	23

#	Article	IF	CITATIONS
109	Dynamic Protein Corona of Gold Nanoparticles with an Evolving Morphology. ACS Applied Materials & Interfaces, 2021, 13, 58238-58251.	8.0	23
110	Mechanistic Insights from Discrete Molecular Dynamics Simulations of Pesticide–Nanoparticle Interactions. Environmental Science & Technology, 2017, 51, 8396-8404.	10.0	22
111	Ultrasmall Molybdenum Disulfide Quantum Dots Cage Alzheimer's Amyloid Beta to Restore Membrane Fluidity. ACS Applied Materials & Interfaces, 2021, 13, 29936-29948.	8.0	22
112	A Framework of Paracellular Transport via Nanoparticlesâ€Induced Endothelial Leakiness. Advanced Science, 2021, 8, e2102519.	11.2	22
113	Structure–Function Relationship of PAMAM Dendrimers as Robust Oil Dispersants. Environmental Science & Technology, 2014, 48, 12868-12875.	10.0	21
114	A Thermodynamics Model for the Emergence of a Stripeâ€like Binary SAM on a Nanoparticle Surface. Small, 2015, 11, 4894-4899.	10.0	21
115	Probing the modulated formation of gold nanoparticles–beta-lactoglobulin corona complexes and their applications. Nanoscale, 2017, 9, 17758-17769.	5.6	21
116	Zinc-coordination and C-peptide complexation: a potential mechanism for the endogenous inhibition of IAPP aggregation. Chemical Communications, 2017, 53, 9394-9397.	4.1	21
117	Probing protein aggregation using discrete molecular dynamics. Frontiers in Bioscience - Landmark, 2008, Volume, 4795.	3.0	21
118	Predicting Binding Affinity of CSAR Ligands Using Both Structure-Based and Ligand-Based Approaches. Journal of Chemical Information and Modeling, 2013, 53, 1915-1922.	5.4	20
119	Brushed polyethylene glycol and phosphorylcholine for grafting nanoparticles against protein binding. Polymer Chemistry, 2016, 7, 6875-6879.	3.9	20
120	CSAR Benchmark of Flexible MedusaDock in Affinity Prediction and Nativelike Binding Pose Selection. Journal of Chemical Information and Modeling, 2016, 56, 1042-1052.	5.4	20
121	New Models of Tetrahymena Telomerase RNA from Experimentally Derived Constraints and Modeling. Journal of the American Chemical Society, 2012, 134, 20070-20080.	13.7	19
122	Thermo- and pH-responsive fibrillization of squid suckerin A1H1 peptide. Nanoscale, 2020, 12, 6307-6317.	5.6	19
123	RNA Tertiary Structure Analysis by 2′-Hydroxyl Molecular Interference. Biochemistry, 2014, 53, 6825-6833.	2.5	17
124	Probing Interdomain Linkers and Protein Supertertiary Structure In Vitro and in Live Cells with Fluorescent Protein Resonance Energy Transfer. Journal of Molecular Biology, 2021, 433, 166793.	4.2	17
125	Labeling native bacterial RNA in live cells. Cell Research, 2014, 24, 894-897.	12.0	15
126	Structure modeling of RNA using sparse NMR constraints. Nucleic Acids Research, 2017, 45, 12638-12647.	14.5	15

#	Article	IF	CITATIONS
127	Human Plasma Protein Corona of Aβ Amyloid and Its Impact on Islet Amyloid Polypeptide Cross-Seeding. Biomacromolecules, 2020, 21, 988-998.	5.4	15
128	Ensemble switching unveils a kinetic rheostat mechanism of the eukaryotic thiamine pyrophosphate riboswitch. Rna, 2021, 27, 771-790.	3.5	15
129	Statistical Analysis of SHAPE-Directed RNA Secondary Structure Modeling. Biochemistry, 2013, 52, 596-599.	2.5	14
130	Direct Observation of β-Barrel Intermediates in the Self-Assembly of Toxic SOD1 _{28–38} and Absence in Nontoxic Glycine Mutants. Journal of Chemical Information and Modeling, 2021, 61, 966-975.	5.4	14
131	Graphene quantum dots obstruct the membrane axis of Alzheimer's amyloid beta. Physical Chemistry Chemical Physics, 2021, 24, 86-97.	2.8	14
132	Discrete Molecular Dynamics Simulation of Biomolecules. Biological and Medical Physics Series, 2012, , 55-73.	0.4	13
133	αB-Crystallin Chaperone Inhibits Aβ Aggregation by Capping the β-Sheet-Rich Oligomers and Fibrils. Journal of Physical Chemistry B, 2020, 124, 10138-10146.	2.6	13
134	Identifying Importance of Amino Acids for Protein Folding from Crystal Structures. Methods in Enzymology, 2003, 374, 616-638.	1.0	12
135	Lysophosphatidylcholine modulates the aggregation of human islet amyloid polypeptide. Physical Chemistry Chemical Physics, 2017, 19, 30627-30635.	2.8	12
136	The Membrane Axis of Alzheimer's Nanomedicine. Advanced NanoBiomed Research, 2021, 1, 2000040.	3.6	12
137	Out-of-Equilibrium Biophysical Chemistry: The Case for Multidimensional, Integrated Single-Molecule Approaches. Journal of Physical Chemistry B, 2021, 125, 10404-10418.	2.6	9
138	Integrative structural dynamics probing of the conformational heterogeneity in synaptosomal-associated protein 25. Cell Reports Physical Science, 2021, 2, 100616.	5.6	9
139	Hydrophobic/Hydrophilic Ratio of Amphiphilic Helix Mimetics Determines the Effects on Islet Amyloid Polypeptide Aggregation. Journal of Chemical Information and Modeling, 2022, 62, 1760-1770.	5.4	9
140	Structural and energetic determinants of tyrosylprotein sulfotransferase sulfation specificity. Bioinformatics, 2014, 30, 2302-2309.	4.1	7
141	Computational Evaluation of Protein Stability Change upon Mutations. Methods in Molecular Biology, 2010, 634, 189-201.	0.9	7
142	Deviation from the Unimolecular Micelle Paradigm of PAMAM Dendrimers Induced by Strong Interligand Interactions. Journal of Physical Chemistry C, 2015, 119, 19475-19484.	3.1	6
143	SAMase of Bacteriophage T3 Inactivates Escherichia coli's Methionine <i>S</i> -Adenosyltransferase by Forming Heteropolymers. MBio, 2021, 12, e0124221.	4.1	5
144	Morphological Determinants of Carbon Nanomaterial-Induced Amyloid Peptide Self-Assembly. Frontiers in Chemistry, 2020, 8, 160.	3.6	4

#	Article	IF	CITATIONS
145	A buried glutamate in the cross-β core renders β-endorphin fibrils reversible. Nanoscale, 2021, 13, 19593-19603.	5.6	4
146	Multiscale Modeling of RNA Structure and Dynamics. Nucleic Acids and Molecular Biology, 2012, , 167-184.	0.2	3
147	The capricious electrostatic force: Revealing the signaling pathway in integrin α2-l domain. Journal of Theoretical and Computational Chemistry, 2018, 17, 1840001.	1.8	3
148	A hidden aggregationâ€prone structure in the heart of hypoxia inducible factor prolyl hydroxylase. Proteins: Structure, Function and Bioinformatics, 2016, 84, 611-623.	2.6	2
149	Amyloidosis: Mitigation of Amyloidosis with Nanomaterials (Adv. Mater. 18/2020). Advanced Materials, 2020, 32, 2070146.	21.0	2
150	Nonnative Energetic Frustrations in Protein Folding at Residual Level: A Simulation Study of Homologous Immunoglobulin-like β-Sandwich Proteins. International Journal of Molecular Sciences, 2018, 19, 1515.	4.1	1
151	Peptide Selfâ€Assembly: Amyloid Selfâ€Assembly of hIAPP8â€20 via the Accumulation of Helical Oligomers, αâ€Helix to βâ€Sheet Transition, and Formation of βâ€Barrel Intermediates (Small 18/2019). Small, 2019, 15, 1970093.	10.0	1
152	Substoichiometric Inhibition of Insulin against IAPP Aggregation Is Attenuated by the Incompletely Processed N-Terminus of proIAPP. ACS Chemical Neuroscience, 2022, 13, 2006-2016.	3.5	1
153	Rational Design of a Ligand-Controlled Protein Conformational Switch. Biophysical Journal, 2013, 104, 18a-19a.	0.5	0
154	Striped Nanoparticles: A Thermodynamics Model for the Emergence of a Stripeâ€like Binary SAM on a Nanoparticle Surface (Small 37/2015). Small, 2015, 11, 4798-4798.	10.0	0
155	Multiscale Modeling of Dendrimers for Biological Applications. Biophysical Journal, 2016, 110, 546a.	0.5	0
156	Brushed Polyethylene Glycol and Phosphorylcholine as Promising Grafting Agents against Protein Binding. Biophysical Journal, 2017, 112, 350a.	0.5	0
157	Mesoscopic Properties and Molecular Mechanisms of IAPP Amyloid Inhibition and Remodeling with Small Molecules. Biophysical Journal, 2017, 112, 340a.	0.5	0
158	Dynamic Equilibrium of the TPP Riboswitch as Observed by MFD Fret. Biophysical Journal, 2017, 112, 368a.	0.5	0
159	Oligomerization and Fibrillization Dynamics of Amyloid Peptides and BETA-Barrel Oligomer Intermediates. Biophysical Journal, 2018, 114, 227a-228a.	0.5	0
160	Transient Interactions in Multidomain Proteins Identified by FRET. Biophysical Journal, 2018, 114, 565a.	0.5	0
161	Effect of Bio-molecules on Human Islet Amyloid Polypeptide Aggregation, Fibril Remodeling and Cytoxicity. Biophysical Journal, 2018, 114, 228a.	0.5	0

162 Amyloid Beta Pathogenesis: Accelerated Amyloid Beta Pathogenesis by Bacterial Amyloid FapC (Adv. Sci.) Tj ETQq0 0.0 rgBT /Overlock 10

#	Article	IF	CITATIONS
163	Interdomain Dynamics Underlie Function and Regulation of Postsynaptic Density Protein 95. Biophysical Journal, 2020, 118, 336a.	0.5	Ο
164	Dynamic Organization in the Supertertiary Structure of PDZ3-SH3-GuK Core Supramodule of PSD-95 Scaffold Protein. Biophysical Journal, 2020, 118, 206a.	0.5	0
165	Quantitative Fluorescence Quenching by Aromatic Amino Acids. Biophysical Journal, 2020, 118, 472a.	0.5	Ο
166	Integrative Structural Dynamics Probing of the Conformational Heterogeneity in Synaptosomal-Associated Protein 25. SSRN Electronic Journal, 0, , .	0.4	0
167	Accelerated Amyloid Beta Pathogenesis by Bacterial Amyloid FapC. Biophysical Journal, 2021, 120, 31a.	0.5	Ο
168	PostÂtranslational Modifications Promote Formation of SOD1 Oligomers With Potential Toxicity in ALS. FASEB Journal, 2015, 29, 564.1.	0.5	0